EVLA Memo 209
JVLA Antenna Absolute Polarization Characteristics at L, S, C, X, and Ku Bands

Rick Perley, Eric Greisen, Wes Grammer, and Rob Long

July 7, 2020

Abstract

Absolute VLA antenna cross-polarizations have been determined on four dates spanning 2011 through 2020, for L through Ku bands (although not all bands were observed on all dates), using the 'receiver rotation' method. Antenna polarizations at X and Ku bands meet the design goal of $\leq$5% over most of the frequency bands for nearly all antennas. Antenna polarizations at L, S, and C bands are higher, generally near 5% over most of these bands. The long-term stability of the polarizers is very good – most changing by less than 1% over eight years. Comparison of antenna polarizations for receivers which have been moved to a different antenna shows that the great majority of the antenna on-axis polarization is due to the receiver, and not the antenna. The excellent long-term stability strongly suggests that polarimetric calibration for most science observations does not require a special calibration regimen, but could utilize tabled values for the cross-polarization corrections.

1 Introduction

The antennas and receivers utilized in radio astronomical observations are polarimetrically impure. In the simplest terms, this means that the antenna outputs labelled 'R' and 'L' do not provide signals which are correct representations of the RCP and LCP components of the astronomical signal. Rather, they each contain small but significant contributions from the opposite polarization, and hence represent elliptical polarization. The antenna outputs should more realistically be labeled 'REP' and 'LEP'. Correct polarimetric imaging thus requires measurement of, and correction for, these contaminating signals.

These cross-coupled signals are often termed 'leakages', and are mathematically described by 'D' terms[1]. The standard methods of determining the antenna cross-leakages employed by both AIPS and CASA result in values of these 'D' terms relative to a reference antenna. In AIPS, it is assumed that the 'R' channel of the nominated reference antenna is pure – there is zero leakage from the opposite polarization. While sufficient for the large majority of observations requiring polarimetry, this method is not sufficient for high fidelity polarimetry, due to incorrect corrections in the higher-order products between the 'D' and polarization terms (D*Q and D*U). Sault and Perley, in EVLA Memos #170 and #177 estimated the dynamic range at which the absolute cross-polarization terms, and full polarization matrix corrections, need to be employed, to be 10^3–10^4:1. Few, if any, polarimetric observations have required such fidelity to date, so there has been little effort expended in implementing absolute polarimetry. With the high sensitivity of the JVLA, and the continuing development of larger and more sensitive arrays combined with demanding polarimetric requirements, the need for utilizing 'absolute' cross-channel leakages is strong.

Calculation of the absolute (non-referenced) terms is, however, not as simple as that for the relative ones. Two methods, described in EVLA Memos #131 and # 170, have been tested, and give similar results. The first method requires two observations of a strong unpolarized source, the first of which is with the array in its normal state, the second with at least one antenna rotated by 90 degrees about its boresight[2]. The second method requires observations of a strongly polarized source (3C286 is the best choice) through a wide range of parallactic angle.

[1] A complex number, describing the amplitude and phase of the voltage signal from one polarization leaking into the other

[2] The entire reflecting structure, including the receiver

The first method was tested in 2009 as a 'proof of principle', using the original VLA correlator, and the first seven antennas which had been converted to wide-band feeds at C-band. Use of the old VLA correlator meant that spectral resolution of the results was very poor – 50 MHz. The results were however sufficient to show that the original design EVLA polarizers at C-band was quite poor, and led to a modified design to give better results. The results are in EVLA Memo #131. Subsequent observations at L, S, and C bands in January 2010, again utilizing the initial wideband polarizers and the old VLA correlator, are reported in EVLA Memo #141. These observations led to the realization that a better wideband polarizer design was needed at L and S bands as well. All three bands' receivers were (for the most part) subsequently modifed.

Further observations at L, S C, and X-bands were taken in March 2011, at which time the WIDAR correlator was available, enabling full receiver bandwidth results to be obtained with 2 MHz resolution. By this time, 10 antennas were available at L-band with wideband receivers (three with new design polarizers), 12 antennas at S-band (9 with new design), all antennas at C-band with wideband receivers (but none with the improved polarizers), and 5 antennas at X-band (the remaining ones having the old VLA narrow-band polarizers). The results from these observations are in EVLA Memo #151.

The second method of determining the absolute leakages, using the parallactic angle rotation of 3C286, was utilized in observations taken in March 2013, at L, S, C, and X bands. The results for C and X bands are given in EVLA Memo #170. Finally, in July 2013, the unpolarized source method was repeated at these bands, and the results for C and X bands, compared to the rotate-3C286 method, are in EVLA Memo #178. None of these efforts actually applied the results to the data to demonstrate the expected improvements.

High-fidelity polarimetry will require determination, and application, of absolute D-terms, for observations where the required polarimetric dynamic range exceeds ~ 1000. In 2019, science observations of 3C273 at X through Q bands with the JVLA, whose goals include high-fidelity polarimetry, and the resulting polarization images are much worse than images of this source taken in the late 1970s with the original VLA. Why so? Two things have changed between the original and the recent observations – the fractional polarization of the nucleus in 3C273 has dramatically increased (from about 2% to nearly 10%), and the high-purity, narrow-band polarizers of the original VLA have been replaced with wide-band polarizers whose leakages are a few times worse. As the higher-order terms in the polarimetric equations involve products of the fractional polarization multiplied by the antenna leakage terms, there is strong suspicion that the failure to fully apply absolute leakage terms is the root cause of the poor polarimetric results.

This situation has encouraged a review of the JVLA polarimetric methodology, and has resulted in a new campaign to determine – and properly apply – the absolute D terms. Included in this new campaign are observations using both methods, so the results can be compared.

This memo gives the results of the determination of the absolute terms, using the 'receiver rotation' method, from all four wideband data sets taken from March 2011 through January 2020. The analysis includes determination of the stability of these polarizers over the 9-year span.

Results from the alternate method of observing 3C286 through meridian transit, which were made at all bands from L through Q, will be given in a subsequent memo.

2 Interferometer Response to Polarized Signals

Brief descriptions of the methods used to determine the absolute leakages are given in Memos #131 and #178. Here we give a more general treatment.

In general, the four complex correlator products ('visibilities') from any pair of arbitarily polarized antennas due to arbitarily polarized radiation are weighted sums of the four Stokes visibilities, with the four coefficients of each sum being functions of the polarization states, as characterized by the 'D' terms, of the two component antennas. The most general form of the visibilities are given below

$$\begin{aligned} V_{r_1r_2} &= \frac{1}{2}G_{r1}G^*_{r2}e^{-i\Delta\Psi}\{(\mathcal{I}+\mathcal{V}) + e^{2i\Delta\Psi}D_{lr1}D^*_{lr2}(\mathcal{I}-\mathcal{V}) \\ &\quad + e^{-2i\Psi_2}D^*_{lr2}(\mathcal{Q}+i\mathcal{U}) + e^{2i\Psi_1}D_{lr1}(\mathcal{Q}-i\mathcal{U})\} \qquad (1) \\ V_{l_1l_2} &= \frac{1}{2}G_{l1}G^*_{l2}e^{i\Delta\Psi}\{e^{-2i\Delta\Psi}D_{rl1}D^*_{rl2}(\mathcal{I}+\mathcal{V}) + (\mathcal{I}-\mathcal{V}) \\ &\quad + e^{-2i\Psi_1}D_{rl1}(\mathcal{Q}+i\mathcal{U}) + e^{2i\Psi_2}D^*_{rl2}(\mathcal{Q}-i\mathcal{U})\} \qquad (2) \\ V_{r_1l_2} &= \frac{1}{2}G_{r1}G^*_{l2}e^{-i\Sigma\Psi}\{e^{2i\Psi_2}D^*_{rl2}(\mathcal{I}+\mathcal{V}) + e^{2i\Psi_1}D_{lr1}(\mathcal{I}-\mathcal{V}) \end{aligned}$$

$$+ (\mathcal{Q} + i\mathcal{U}) + e^{2i\Sigma\Psi} D_{lr1} D^*_{rl2}(\mathcal{Q} - i\mathcal{U})\} \tag{3}$$

$$V_{l_1 r_2} = \frac{1}{2} G_{l1} G^*_{r2} e^{i\Sigma\Psi}\{e^{-2i\Psi_1} D_{rl1}(\mathcal{I} + \mathcal{V}) + e^{-2i\Psi_2} D^*_{lr2}(\mathcal{I} - \mathcal{V})$$

$$+ e^{-2i\Sigma\Psi} D_{rl1} D^*_{lr2}(\mathcal{Q} + i\mathcal{U}) + (\mathcal{Q} - i\mathcal{U})\} \tag{4}$$

where $\Sigma\Psi = \Psi_1 + \Psi_2$ and $\Delta\Psi = \Psi_1 - \Psi_2$ are the sum and differences of the antenna orientation angles w.r.t. the astronomical sky. The antenna orientation is given by the antenna's parallactic angle plus any peculiar orientation of the antenna w.r.t the sky. For the VLA, which was designed such that all antennas have the same parallactic angle[3], and whose receivers are designed to be aligned identically with the antennas, these orientation angles are the same for each antenna, and are given by the parallactic angle alone[4]. The $\mathcal{I}$, $\mathcal{Q}$, $\mathcal{U}$, and $\mathcal{V}$ are the complex visibilities of the source, which are related to the surface brightnesses in I, Q, U, and V by Fourier transform. The $\mathcal{G}$ terms are the voltage gains for the two polarization channels. The D terms describe the voltage coupling between the two polarization channels. The subscripts describe the coupled pair, and the antenna number. Hence, D_{rl1} describes the amplitude and phase of the RCP signal which is coupled to the LCP channel for the first antenna. These coefficients are directly related to the antenna's polarization ellipse, as described in the appendix.

These rather fearsome-looking equations are considerably simplified for the case of radiation from an unresolved and unpolarized source located at the phase tracking center as seen by two antennas whose parallactic angles are the same. In this case, the complex visibilities can be replaced by the scalars representing the point-source flux. Presume now that the parallel hand gains, including the multiplicative phase terms adjacent to the parallel hand gains in equations 1 to 4, have been applied [5], and that the correlations have been divided by the total intensity value, so the visibility values are normalized. The equation set then simplifies to

$$V_{r_1 r_2} = (1 + D_{lr1} D^*_{lr2})/2 \tag{5}$$

$$V_{l_1 l_2} = (1 + D_{rl1} D^*_{rl2})/2 \tag{6}$$

$$V_{r_1 l_2} = (D_{lr1} + D^*_{rl2})/2 \tag{7}$$

$$V_{l_1 r_2} = (D_{rl1} + D^*_{lr2})/2. \tag{8}$$

Now suppose the second antenna has been rotated by an angle θ, and that another observation of an unpolarized, unresolved source made. The resulting equation set becomes

$$V^R_{r_1 r_2} = (1 + e^{2i\theta} D_{lr1} D^*_{lr2})/2 \tag{9}$$

$$V^R_{l_1 l_2} = (1 + e^{-2i\theta} D_{rl1} D^*_{rl2})/2 \tag{10}$$

$$V^R_{r_1 l_2} = (D_{lr1} + e^{2i\theta} D^*_{rl2})/2 \tag{11}$$

$$V^R_{l_1 r_2} = (D_{rl1} + e^{-2i\theta} D^*_{lr2})/2. \tag{12}$$

where the 'R' superscript denotes that the second antenna has been rotated. The four equations for the cross-products (eqn 7, 8, 11 and 12) are easily combined to provide the leakage terms:

$$D_{rl1} = \frac{2(V^R_{l1r2} - e^{-2i\theta} V_{l1r2})}{1 - e^{-2i\theta}} \tag{13}$$

$$D_{lr1} = \frac{2(V^R_{r1l2} - e^{2i\theta} V_{r1l2})}{1 - e^{2i\theta}} \tag{14}$$

$$D^*_{lr2} = \frac{2(V_{l1r2} - V^R_{l1r2})}{1 - e^{-2i\theta}} \tag{15}$$

$$D^*_{rl2} = \frac{2(V_{r1l2} - V^R_{r1l2})}{1 - e^{2i\theta}} \tag{16}$$

The relationships become particularly simple when $\theta = \pm\pi/2$:

$$D_{rl1} = V^R_{l1r2} + V_{l1r2} \tag{17}$$

[3] by tilting the antenna pads so that all antennas' azimuth axes are parallel

[4] In fact, it is now known that the plane of the VLA's antenna pads are not all parallel, but the effect of this on the polarimetry is not yet well understood. See Frank Schinzel's EVLA Memo#205 for a discussion.

[5] We gloss over the problem of how to precisely determine these gains, given that the parallel hand correlations, which are needed for this determination, are themselves functions of the polarization of both the source and antennas.

$$D_{lr1} = V^R_{r1l2} + V_{r1l2} \tag{18}$$
$$D^*_{lr2} = V_{l1r2} - V^R_{l1r2} \tag{19}$$
$$D^*_{rl2} = V_{r1l2} - V^R_{r1l2} \tag{20}$$

Note that these relations are independent of the orientation of the antennas – intuitively obvious since the presumption of zero polarization means there are no preferred angles on the sky. Note that both AIPS and CASA use a different normalization convention, such that the relations in equations 5 through 12 are multiplied by two, while those in equations 13 through 20 are divided by two.

3 The JVLA's Polarizers

The JVLA utilizes circularly polarized receivers at all bands except P. The justification for the additional engineering effort required is that this considerably simplifies the calibration process, as the parallel-hand correlations, which are utilized for gain calibration, are (nearly) insensitive to the linearly polarized signals of the calibrator sources. This is an important advantage, since nearly all of the calibrators utilized by the VLA are polarized at levels of a few percent. Furthermore, nearly all have time-variable polarization, with timescales varying from weeks to years. Although the calibrator polarizations can be determined from the science observations, this is generally not feasible for short (snapshot) observations. Hence, the advantage of being able to ignore the polarization state of the calibrators through the use of circularly polarized feeds is a real one.

Producing receiver outputs proportional to the circularly polarized components of the incoming electric field requires combining the linearly polarized components with 90 degree phase shifts. This is accomplished in different ways for each of the bands.

At L, S, and C bands, the circular components are generated by a quadridge OMT (ortho-mode transducer) which produces outputs proportional to the orthogonal linearly-polarized components of the incoming signal, directly followed by a quadrature hybrid 4-port coupler. These devices and are cooled to 15K in the receiver dewer to minimize their contributions to the system temperature.

EVLA Memo #151 noted that the initial choices for the quadrature hybrids (they are commercial devices) for the EVLA at these bands were designed for room-temperature operation, whose performance degraded significantly upon cooling to cryogenic temperatures. A modified design was implemented, which proved to be more stable, with most receivers subsequently retrofitted.

At X band, the 90 degree phase shifts are introduced prior to the OMT by a corrugated waveguide phase shifter, so the outputs of the quadridge OMT are proportional to the circular polarized components of the incoming signal. At Ku, K, and Ka-bands, a similar waveguide phase shifter is followed by Boifot junction OMT. The corrugated waveguide phase shifters employed at these bands have quite different performance characteristics from the quadrature hybids, as shown in the following sections.

4 Observations

All observations reported here use the 'rotate one antenna' method. Unfortunately, it is not possible to rotate an VLA antenna about its boresight axis. However, the receivers can be rotated by multiples of 45 degrees, as they are mounted to the horn by 8 bolts uniformly distributed around the flanges. Provided that the polarization leakages are dominated by the receiver and polarizer, the antenna cross-polarizations can be determined by receiver rotation alone. We show in Section 6 that the receiver polarizations do indeed dominate the total polarization.

Wide-band, full spectral resolution observations with the VLA, utilizing the WIDAR correlator, were taken in four epochs. The details are described below:

- **March 2011**. Observations were made of 3C147 (J0542+4951) on 9, 10, and 11 March 2011 at L, S, C, and X bands, with the array in the B configuration. The receivers on ea06 were rotated on 10 March by 90 degrees for each of these bands. These results are of limited use for this study, as most of the polarizers at that time were of an older design, and have subsequently been replaced. Furthermore, the source 3C147, although of negligible polarization at L and S bands, becomes slightly polarized (few percent) at C and X bands, which will compromise the results.

- **July 2013**. Observations were made of 3C147, 3C138 (J0521+1638), and 3C84 (J0319+4130) on 23 July, 2013 at L, S, C and X bands, on 23 July 2013, with the array in the C configuration. The initial observations, in the 'normal' state were taken in the morning, after which the receivers on ea26 were rotated by 90 degrees. 3C84 is very strong (more than 30 Jy), and known to be unpolarized at these bands. The inclusion of 3C138 permitted the correct phase relation between the polarized channels to be determined. The array was fully outfitted with EVLA wide-band receivers, although the polarizers for many of the antennas at L, S, and C bands were of an older design which were subsequently replaced.

- **February 2019** Observations were made of 3C147 and OQ208 (J1407+2827) on February 5, 6, 7, and 8, 2019 at L, S, C, X, and Ku bands, with the array in the C configuation. Recent observations show that OQ208 is unpolarized to a level of less than 0.2% at these bands. The receivers at L, S, and C bands on ea10 were rotated by 90 degrees on February 8. It was not possible to rotate the X and Ku band receivers in the time available, so the results are necessarily limited to L, S, and C bands. The absence of a strongly polarized source means the R-L phase can not be determined from these observations. Comparison of the antenna polarizations between 2019 and 2020 enabled this offset to be determined, as described below.

- **January 2020** Observations at L, S, C, X and Ku bands were made of 3C147, 3C286 (J1331+3030), OQ208, and 3C84 on Jan 26, 29, and 30, 2020, with the array in the D configuration. The addition of 3C286 allowed establishment of the correct phase difference between the R and L signal channels, while 3C84 was added as the target unpolarized source at X and Ku bands, due to the low flux density of OQ208 at these bands. Antenna ea09 was rotated by 90 degrees at L, S, C and Ku bands, and by -45 degrees (CCW, as seen from above), due to physical limitations at X band, on Jan 26 and 29. The 'rotated' state observations were repeated on the 29th, as one of the IF channels of ea09 (the critical rotated antenna) was not functioning on the 26th.

Data were calibrated with standard methods, using the `AIPS` data reduction software package. By far the most laborious task in the calibration process is to remove the RFI. As the RFI affects the gains, and the gains are needed to correctly flag the data, the process of RFI removal is necessarily iterative. Channels and spectral windows deemed unrecoverable (by visual inspection through SPFLG and UVPLT) were removed entirely with UVFLG. Sporadic RFI was removed via CLIP. The 2013 and 2020 data were polarization-calibrated using the zero-polarization source option. This permitted setting of the cross-hand phases using the 3C286 or 3C138 observations. The cross-hand phases for the 2019 observations (which did not include a known polarized source) were found by comparison to the 2020 results for the stable antennas. Note that the polarization calibration was done only to enable determination of the cross-hand phases – these polarization solutions were not utilized in the subsequent determination of the absolute polarizations.

The absolute polarization values were determined with the special-built task TRUEP, utilizing the relations shown in equations 13 to 16. The plots shown below, comparing polarizations between different antennas and dates, were made with the special-built task PDPLT.

5 Results – Dependency on Source Polarization and Flux

The method employed requires a strong, unpolarized source. Use of a polarized source will result in an error which rough analysis shows will be comparable to the fractional polarization of the source. As essentially all calibrator sources are linearly polarized, it is important to know at what level the source polarization significantly affects the derived values of the antenna polarizations.

The receiver-rotation method is highly sensitive to source flux, as the D terms for all antennas (except the rotated one) are determined from a single observation, on a single baseline, (the one linking the rotated to the unrotated antennas) and with narrow channelwidth. Hence a very strong, unpolarized source is needed.

To determine these dependencies, we included three sources in the January 2020 X-band observations: 3C84 (J0319+4130), with about 32 Jy flux with polarization less than 0.1%, OQ208 (J1407+2827), which is less than 0.2% linearly polarized, but with only 0.6 Jy at this frequency, and 3C147 (J0542+4951), which is about 2% polarized, and 3.6 Jy at this band.

Shown in Fig 1 are overlays with the solutions for ea09 (the rotated antenna) using 3C84 and OQ208 in the left panel pair, and 3C84 and 3C147 in the right panel pair. The left panel shows the effect of SNR – the blue trace is from 3C84, the red points from OQ208. The two solutions are the same, but the improved SNR from the 3C84 result is dramatic. The right panel shows the effect of using a slightly polarized source – 3C147, which is weakly polarized gives an offset of about 0.4% from that of the completely unpolarized source 3C84 – significantly less than the polarization fraction of 3C147, but enough to skew the results. A conclusion that the target source should be less than 1% polarized seems justified.

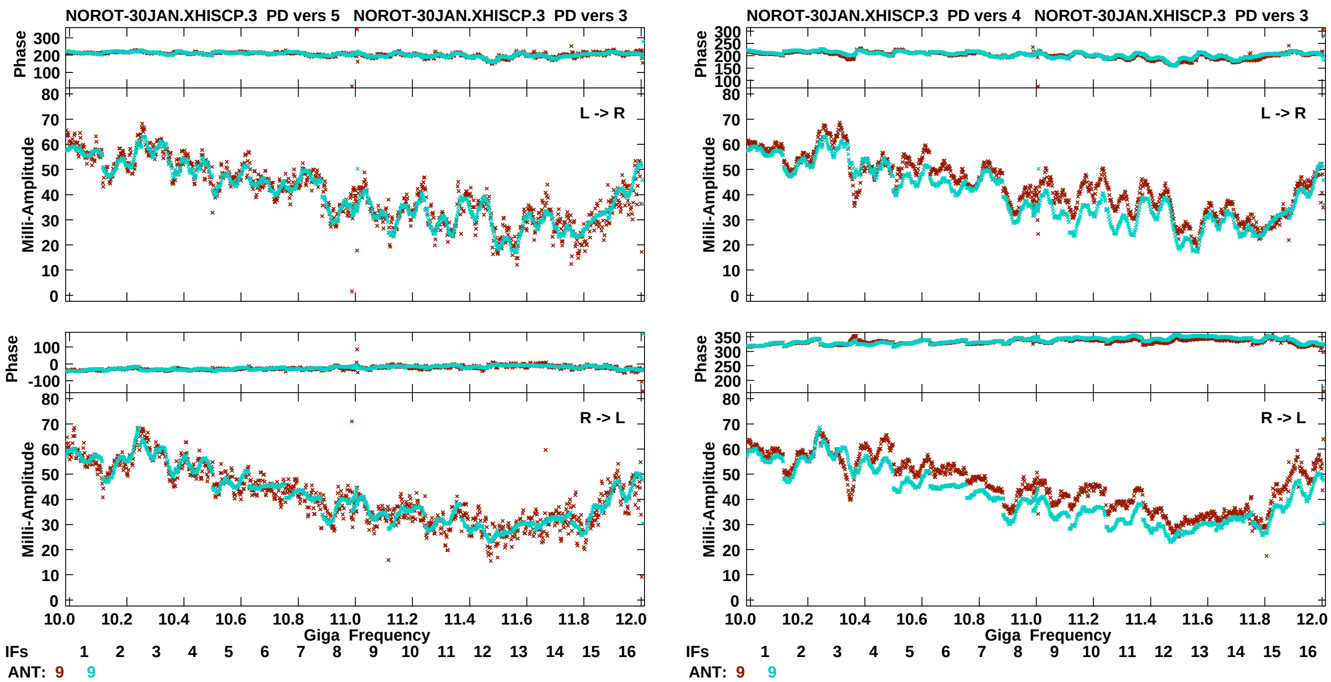

Figure 1: Showing the effect of source flux, and of using a polarized source in determining the absolute polarization of the 'rotated' antenna ea09. In these, and in all subsequent plots, the results are presented as vertically arranged pairs. The top pair shows the amplitude and phase of the signal leaking from the LCP channel to RCP, and bottom pair that from RCP to LCP. Each pair shows the leakage signal phase in degrees on top, and the fractional amplitude leakage, in 'milliunits' – 10 = 1%, below. Here, the left panel pair shows the results using two unpolarized sources of very different flux: The 30Jy source 3C84 (blue), and the 0.4 Jy source OQ208 (red). The right panel pair shows the sensitivity of the result to a polarized source by comparing the unpolarized source 3C84 (blue) and the slightly (2%) polarized source 3C147 (red), also for ea09. There is a small but notable offset of the polarization using the polarized source.

The result shown in Fig 1 is for ea09, for which there are N-1 baselines available to improve the SNR. For the un-rotated antennas, the dependence on source flux is much more critical, as these utilize only the single baseline to the rotated antenna. The dependency is shown in the left panel pair of Fig 2 which shows the leakages of ea04 at X-band, using the 20 Jy source 3C84 (yellow) and the 0.7 Jy source OQ208. We conclude that an unpolarized source of at least 10 Jy is required for results accurate to a fraction of 1%. The right panel shows the short-term stability (repeatibility) of the derived solutions, from observations of 3C84 taken three days apart. There is no discernible difference.

6 Results – Leakages for 2020

In this section, we give a detailed overview of the current state of the JVLA polarizers for all antennas from the January 2020 data for L, S, C, X, and Ku bands. The unpolarized target source utilized for the three lowest frequency bands was 3C147, and 3C84 for the upper two bands.

6.1 L-Band

The L-band polarizations for all available antennas are shown in Fig 3. The gaps from 1.2 to 1.3 GHz, and from 1.55 to 1.6 GHz are due to satellite interference, to which we are particularly vulnerable in the D configuration. The key conclusion for L-band is that the cross-polarization amplitudes are very similar for all antennas in both

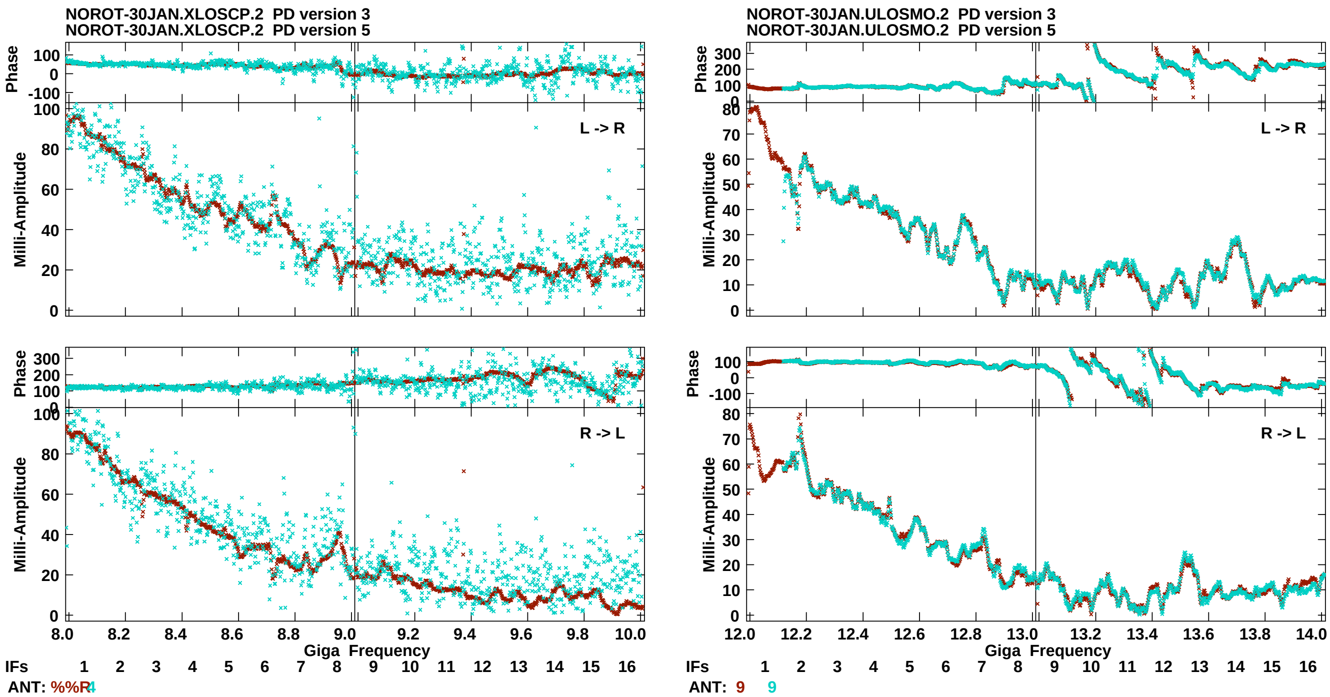

Figure 2: (Left) Showing the effect of signal-to-noise in determining the absolute polarization for ea04 between 8 and 10 GHz. The two sources utilized are both unpolarized to 0.2%. 3C84 (red) is very strong – 30 Jy, while OQ208 (teal) is weak – 0.6 Jy. The solutions are the same, but the effect of the lower SNR for OQ208 is obvious. (Right) Showing the repeatability of the measurement. The red trace is from 3C84 taken on 29 January, the blue trace from 3C84 taken on 26 January. (The first SPW on this day was flagged). The difference is barely discernible.

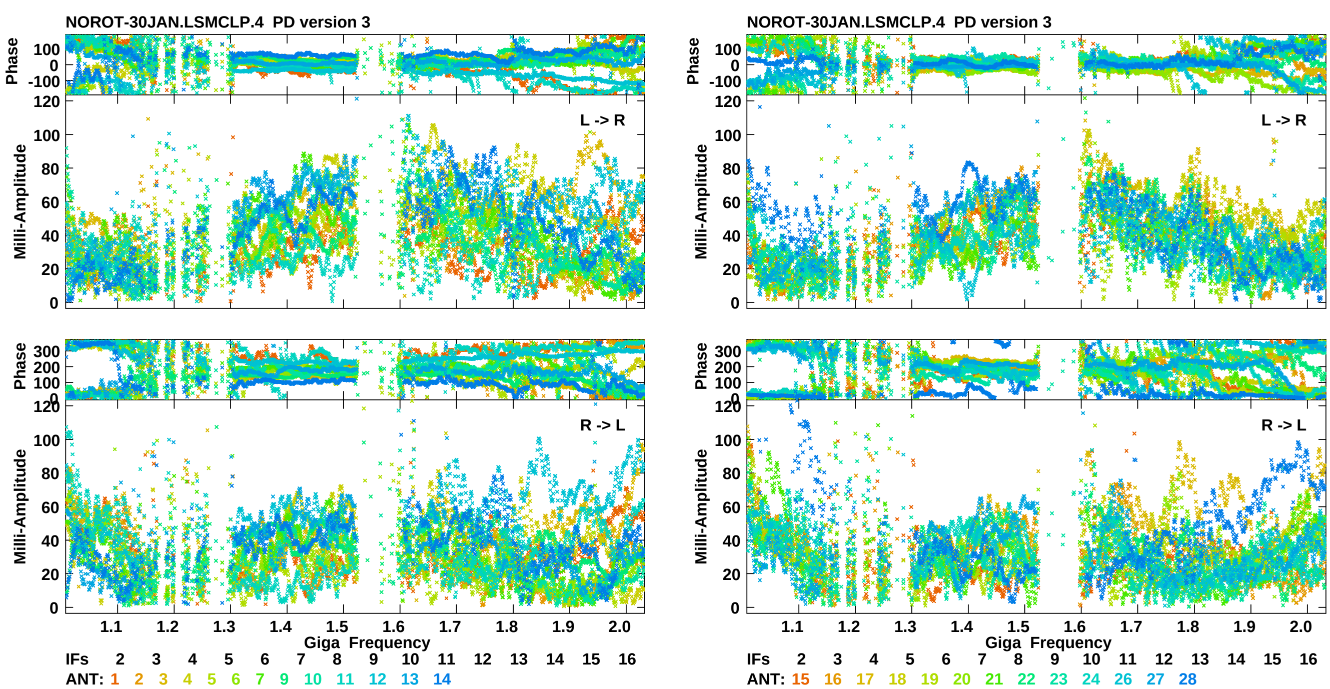

Figure 3: The absolute cross-polarizations of the VLA antennas from 1.0 to 2.0 GHz, from the January 2020 observations. The left panel pair shows antennas 1 through 14, the right panel pair shows antennas 15 to 28. The leakages are very similar amongst the antennas, and of generally low amplitude. The gaps are due to RFI.

amplitude and phase and, with few exceptions, near the design goal of 5% over most of the 1 – 2 GHz band. In general, these cross polarization are ‘convex’, with the maximum near 1.6 GHz. Most antennas have a rise in cross-polarization at frequencies below 1.1 GHz. The $\sim$ 15-MHz fine-scale structure evident in most antennas is due to reflections between the receiver or horn, and the subreflector.

6.2 S-Band

The polarizations for all available S-band receivers are shown in 4. There results show a clear tendency for the polarizers to belong to one of three ‘families’ – showing concave (left), convex (center), or flat behavior (right) as a function of frequency. The ’convex’ and ’flat’ groupings (center and right panels) are quite similar in their characteristics, and we believe them to be of the same design. It is apparent that there are two different

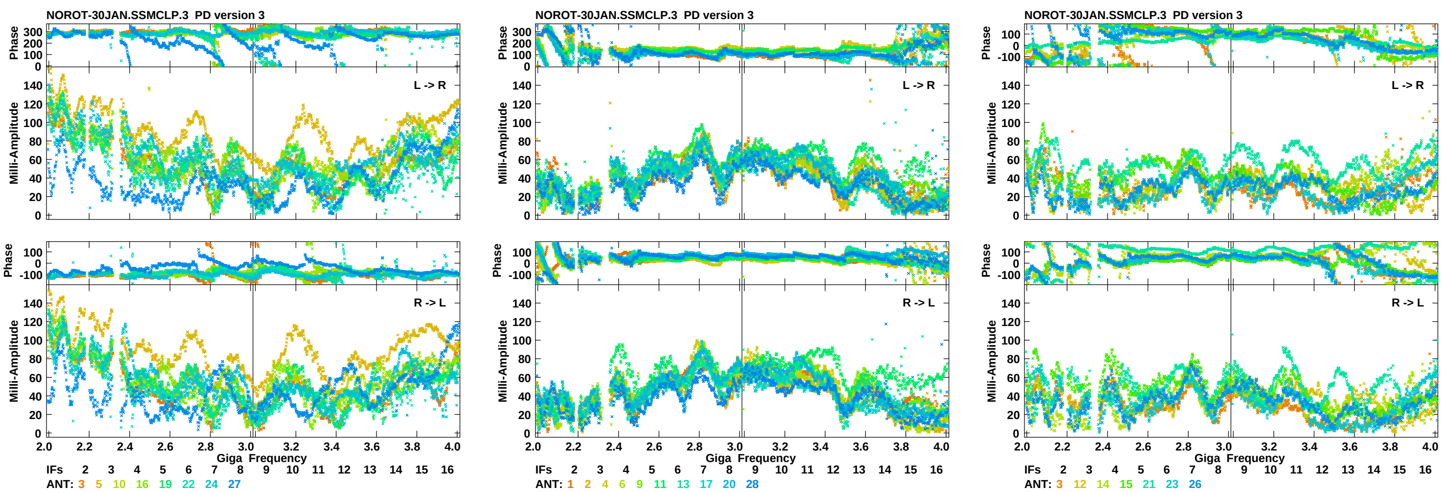

Figure 4: The absolute cross-polarization of the S-band receivers from 2.0 to 4.0 GHz, from the January 2020 observations. Antennas showing concave polarization behavior are on the left, convex behavior in the center, and flat behavior on the right. ea07 (yellow trace in the left panel) has the anomalously high cross-polarization.

designs currently implemented on the array. Antennas ea05, 07, 10, 16, 19, 22, and 24 have the concave shape characteristic of the old EVLA polarizer design. All of the seven receivers in these antennas are among the nine oldest S-band receivers, suggesting that they retain the original hybrid. [6] Examination of the polarization of the antennas in which these seven receivers have subsequently been mounted between 2011 and 2019 show that their polarizations have not appreciably changed since 2011. These ‘older’ designs are problematic because of their higher cross polarization.

In general, the modified design polarizers have considerably better polarization performance than the old, with most meeting the 5% goal over most of the frequency band.

6.3 C-Band

C-band cross-polarizations are shown in Fig 5. As at S-band, there appears to be two different designs in the array. The concave shapes, with higher overall polarization, are from the old design hybrids, and are shown in the upper left panel pair of the figure. The antennas involved are ea05, 15, 25, 26, and 27. However, unlike S-band, the receivers involved are not the oldest. It seems likely they were left out when the retrofits to the new hybrid were done. Unlike S-band, where the change in design occured during the receiver construction phase, all C-band receivers initially utilized the old polarizer design. Comparison of the 2020 polarization to the 2013 polarization, matching antennas with the same receivers to those antennas which now have the apparently ‘old’ polarizers, shows that the polarizations of these five receivers did indeed change. But it appears that these changes did not result in the shape associated with the new hybrids.

[6]The two original receivers not showing concave polarization behavior were clearly modified, as their polarizations changed dramatically before 2019. All receivers built following the original nine had the improved hybrid, except one – S-014. This receiver had the high-polarization ‘concave’ shape in both 2011 and 2013, but was clearly modified prior to 2019 to the modern hybrid.

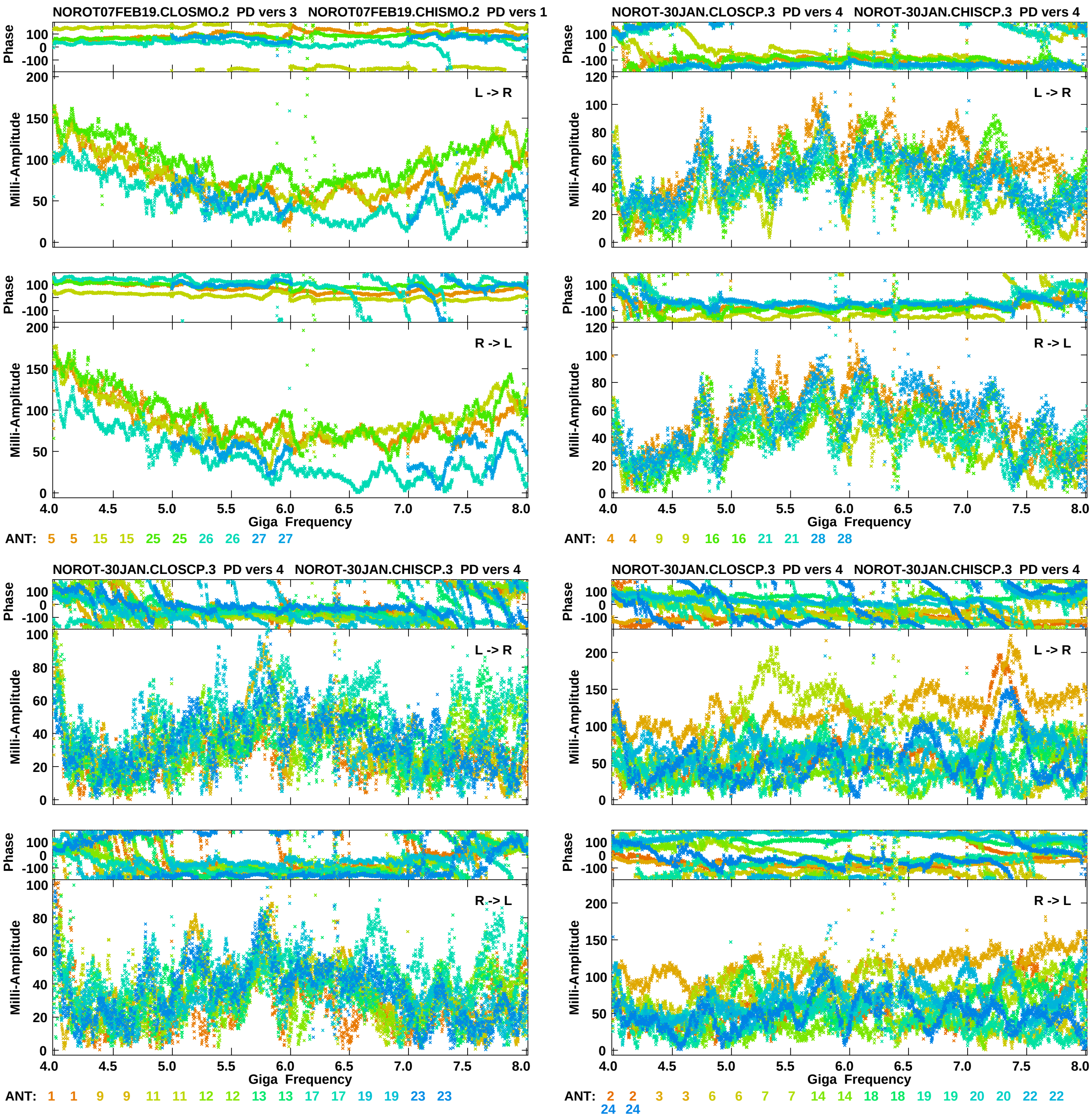

Figure 5: The absolute cross-polarization of the C-band receivers from 4 to 8 GHz, from the January 2020 observations. The top left panel pair shows five antennas with 'concave' polarization, suggesting they retain the original design polarizers. The top right and bottom left panel pairs show the antennas with new-design 'convex' polarization. The bottom right shows nine antennas with 'flat' polarizations. Four of these are unusually high: ea02, 03, 07, and 24.

The remaining panels of the figure show the 'new' design polarizers on the rest of the array. The upper right and lower left panels show antennas with the typical 'convex' polarization signature. The bottom right shows antennas with 'flat' polarization, including four whose polarization is well above the design goal – ea02, 03, 07 and 24. Overall, the polarization performance of the 'new' design is better than the 'old', with performance very similar to that seen at both L and S bands.

6.4 X-band

X-band cross-polarizations are shown in Fig 6. The antennas are displayed in two panels – the left panel shows those antennas whose polarization at 8.0 GHz is more than 8.5%, while the right panel shows those whose polarization is less than 8.5% at 8.0 GHz. The polarizers at this band are of a different design than at L, S, and

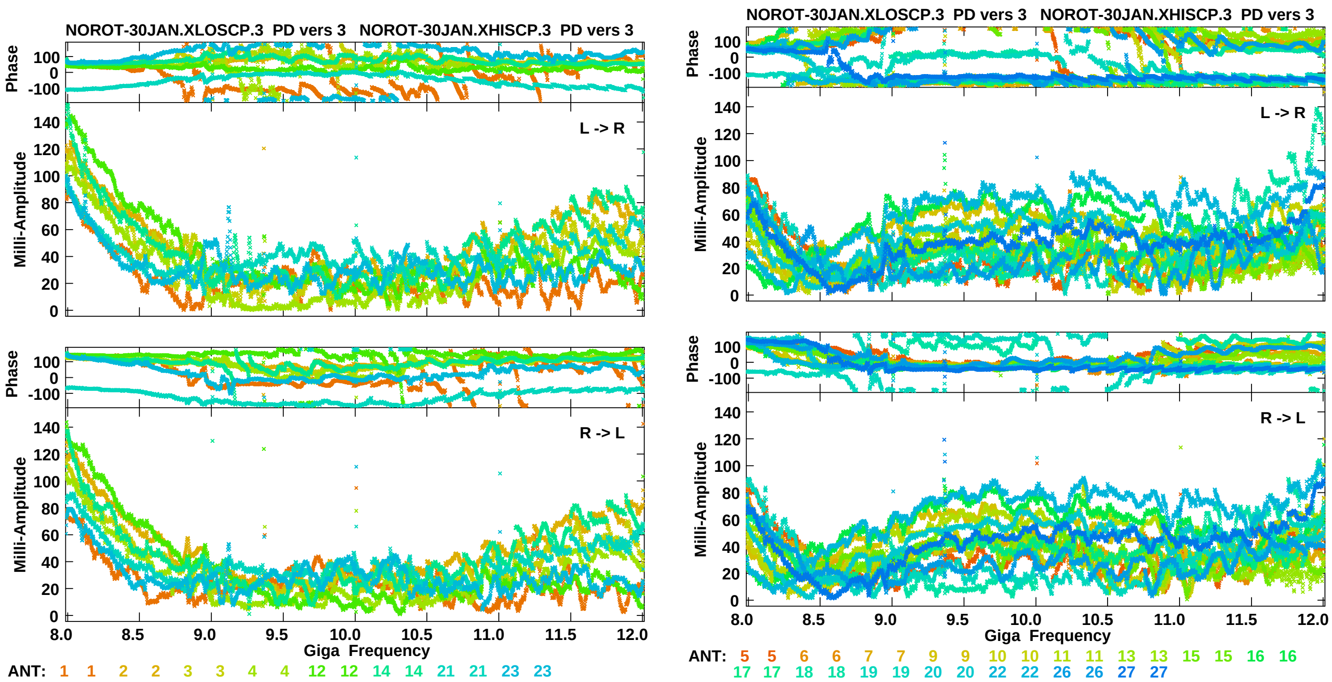

Figure 6: The absolute cross-polarization of the X-band receivers from 4 to 8 GHz, from the January 2020 observations. The antennas whose 8 GHz polarizations are more than 8.5% are shown in the left panel. Those with lower than 8% polarization at 8 GHz are shown in the right panel.

C bands, employing a waveguide phase shifter, before the OMT, to provide the wide-band 90 degree phase shift. The phase shift provided is roughly parabolic as a function of frequency, with the desired 90 degrees reached at two frequencies within the band. This results in a cross-polarization amplitude dependence which is minimized at these two frequencies. These polarization minima (especially that at the lower frequency) are most evident in the right panel. The left panel shows those antennas for which it is clear that the lower frequency is too high, (typically 9 to 9.5 GHz, compared to the $\sim$ 8.5 GHz for the right-panel antennas), resulting in rather high cross-polarization at the bottom end of the band. All antennas have a similar 'shape' to the cross-polarization, and most antennas meet the design goal over most of the frequency range.

6.5 Ku-Band

The Ku-band antenna polarizations are all very similar. Representative plots are shown Fig. 7. Notable here are the 180 phase 'flips' between the middle half of the passband, and the frequencies below and above. These are due to the polarization minima associated with the parabolic phase dependence in the microwave phase shifter. (The notable rapid phase changes in the middle frequencies are due to the leakage minima). Three Ku-band antennas have polarization behaviors quite different than the others. In Fig 8 we show these – ea03 and 13, both of which have extraordinarily high cross polarization at the high end of the band, and ea22, which has a phase 180 degrees different than all other antennas.

These results show that all antennas (with the three exceptions shown above) are very similar, and easily meet the design goal of 5% except for the lowest 500 MHz of the band (12 – 12.5 GHz) for some antennas.

All antennas display strong oscillations in their polarization behavior, to varying degrees. These are likely due to internal reflections in the electronics. With a typical frequency separation of these of $\sim$300 MHz, the free-space equivalent physical separation of the reflection points is $\sim$50 cm.

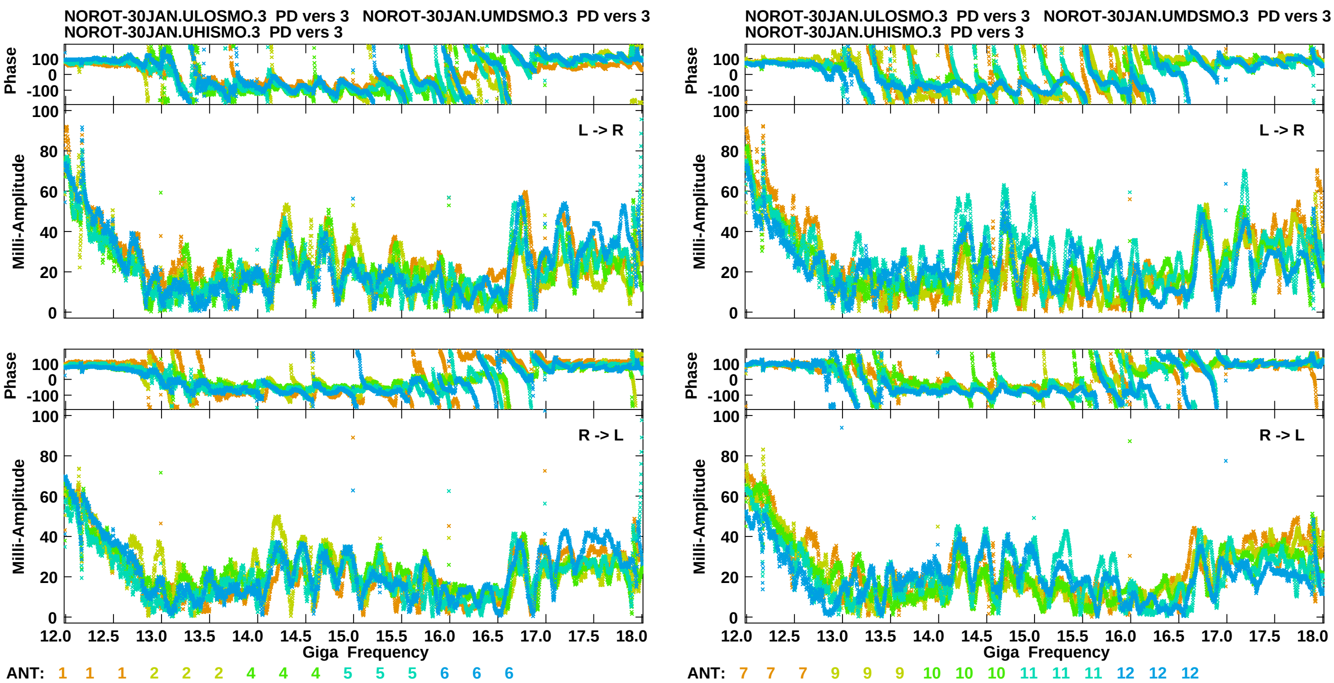

Figure 7: The cross polarizations at Ku-band for ten representative antennas. Ea01, 02, 04, 05 and 06 on the left side, ea07, 09, 10, 11 and 12 on the right. All other antennas are very similar to those shown. Note the 180 phase reversal between the middle half and outer quarters – a result of the phase shifts being more, or less than 90 degrees on each side of the nulls.

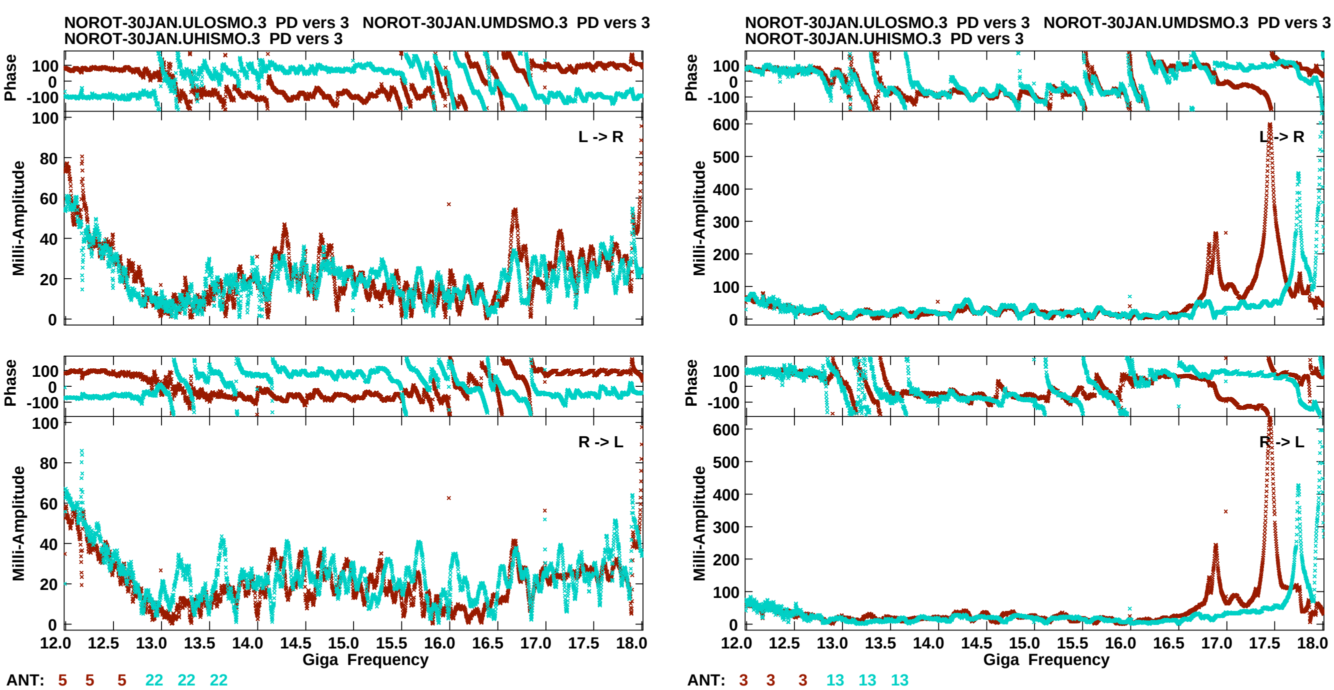

Figure 8: Three antennas with anomalous cross-polarization at Ku-band. On the left side, ea05, which has normal polarization, and ea22, whose amplitude is normal, but whose phases are 180 degees away from all other antennas. On the right side, ea03 and ea13, both of which have extremely high polarization at the high frequency end of the band.

7 Results – Long-Term Stability

Stability of the cross-polarization is a very important characteristic, since if the antenna polarizations are sufficiently constant, characterization of the polarization would not be required for most polarimetry observations, thus saving considerable observing time and calibration effort. In such cases, investigators would use predetermined tables for their polarimetric gain calibration.

Long-term stability is expected, as the structures responsible for the cross-polarization (chiefly the receivers) are isolated in temperature-controlled dewers, isolated from the outside world, and comprised of components with long-term stability.

Related to this issue is the question of what fraction of the (on-axis) polarization is due to the receiver. The antennas are fairly symmetric structures, which leads to an expectation that the on-axis polarization of the antennas alone should be small. Grasp8 simulations by Walter Brisken, (EVLA Memo#58) support this expectation. The hypothesis that the system polarization is dominated by the receivers can be tested with the current data sets, as receivers have been regularly cycled through the antennas, due to maintenance.

These two questions are investigated in the following sections.

7.1 L-band

Nearly all L-band receivers were modified between 2011 and 2019. Six were not modified after 2013, so the long-term stability of the polarization over a six-year span can be determined from these. Two examples are shown in Fig. 9. The left panel pair shows receiver L-011, which was on ea08 in 2013 and 2019, and moved to ea19 by 2020.

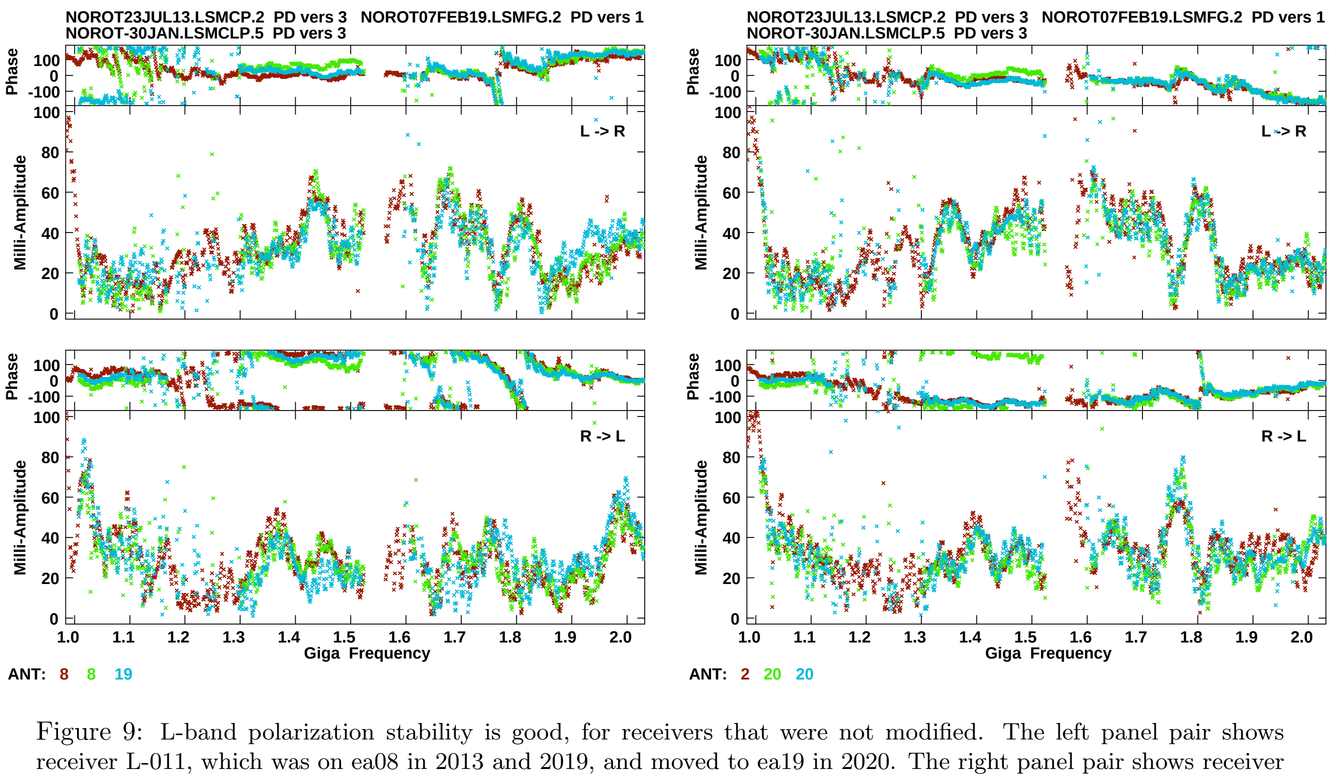

Figure 9: L-band polarization stability is good, for receivers that were not modified. The left panel pair shows receiver L-011, which was on ea08 in 2013 and 2019, and moved to ea19 in 2020. The right panel pair shows receiver L-015, which was on ea02 in 2013, and on ea20 in both 2019 and 2020. These show both that the polarization is stable to ∼1% over long periods of time, and that the polarization characteristics are dominated by the receiver, not the antenna.

The right panel shows receiver L-015, which was on ea02 in 2013, and was on ea20 in both 2019 and 2020. For both plots, the large scale polarization structure remains the same, despite the change of antennas, indicating that these spectral features are determined by the receiver. Additionally, and at all epochs, there is a finer scale structure which is not nearly as stable. These are due to reflections in the signal path, and the frequency scale of ∼ 12 MHz suggests a reflection separation of 15 meters – corresponding to the distance between the OMT and subreflector. This external factor – subject to elevation, weather and temperature differences – is not as stable as the receivers, and clearly limits the repeatability of the polarization stability.

7.2 S-band

Antennas 6 and 26 have kept the same S-band receivers since 2011. In Fig 10 we show the antenna polarization for these two antennas for all four years. Note that there were no changes in cross-polarization greater than 1%

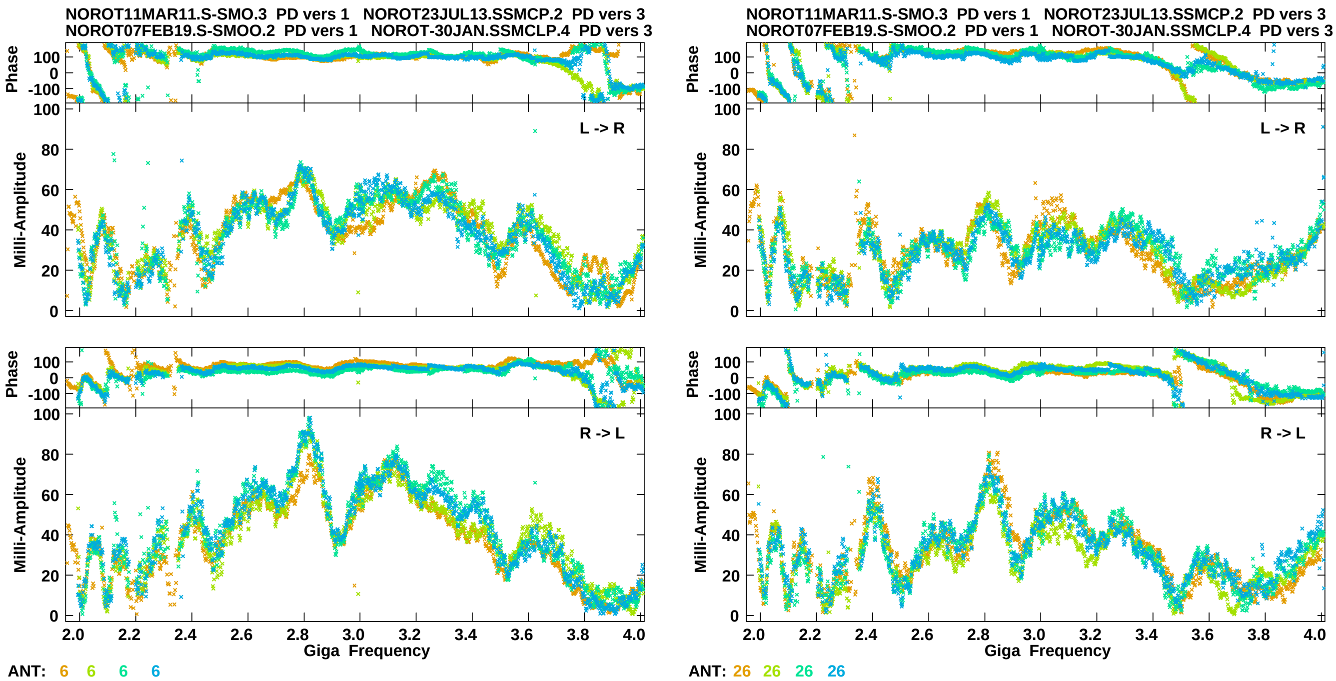

Figure 10: Showing the remarkable polarization stability for two S-band antennas whose receivers have not changed, over the period 2011 to 2020. Ea06 is shown in the left panel pair, ea26 in the right panel pair.

at any frequency from 2011 to 2020, and less than that since 2013.

Due to maintenance and upgrades, receivers have migrated around from antenna to antenna. This gives us an opportunity to check the degree to which the polarization characteristics are determined primarily by the receiver (as expected), or whether there is a significant contribution from the antennas. Figure 11 shows the polarization of three different antennas, at three different times, for which the same receiver (S-008-01) was involved. It will be noted that the polarizations are very similar, despite there being three different antennas involved. Each of the two plots shows the polarization of a unique receiver on two different antennas – the left plot shows receiver S-027 on ea05 in 2013, and on ea27 in 2020. The right plot shows receiver S-011 on ea14 in 2013, and on ea02 in 2020. The polarization amplitudes and phases are closely similar, typically deviating by less than 0.5%, with maximum deviation of less than 2%. Not all receivers are as repeatable as these, when measured on different antennas, but in no case is there an average change more than 1%. In all cases, the large-scale structures (fluctuations on scales more than 100 MHz, thus associated with length scales associated with the receiver) are retained. The conclusion from this is clear – antenna polarizations are dominated by the receivers.

7.3 C-band

All receivers were modified between 2011 and 2019, so we can show here only the stability for the 11 months between February 2019 and January 2020. In general, all antennas whose receivers did not change showed excellent stability. We show in fig 12, the polarization for two antennas, ea05 (left), which has an 'old-style' polarizer, and ea12 (right), with the 'new-style'. (Note the change in scale). The polarizations did not change more than 0.2% in either. This is typical for all antennas.

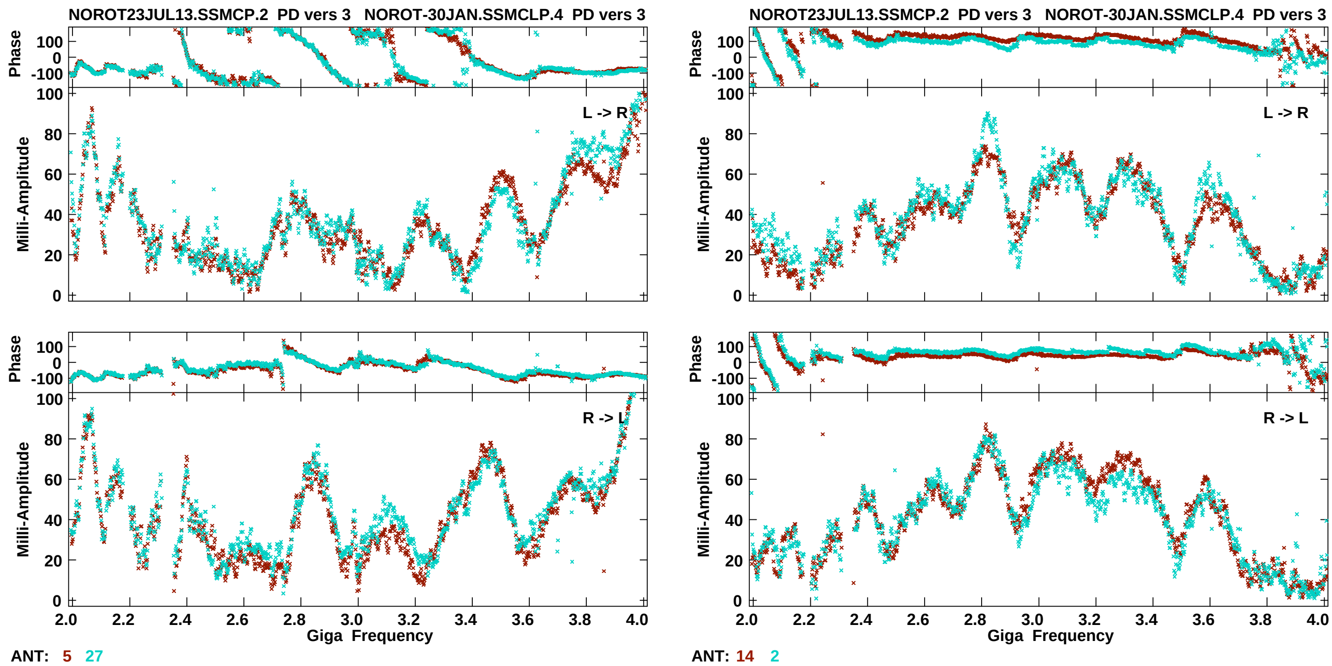

Figure 11: Showing how polarization performance is set largely by the receiver, not the antennas. The left panel pair shows receiver S-027 on two different antennas – ea05 in 2013, and ea27 in 2020. The right panel pair shows the polarization of S-011 in ea14 in 2013, and in ea02 in 2020. Typical changes are ∼0.5%, with maximum deviation of 2%. Nearly all receivers show similar characteristics – the polarization is largely set by the receiver, not the antenna.

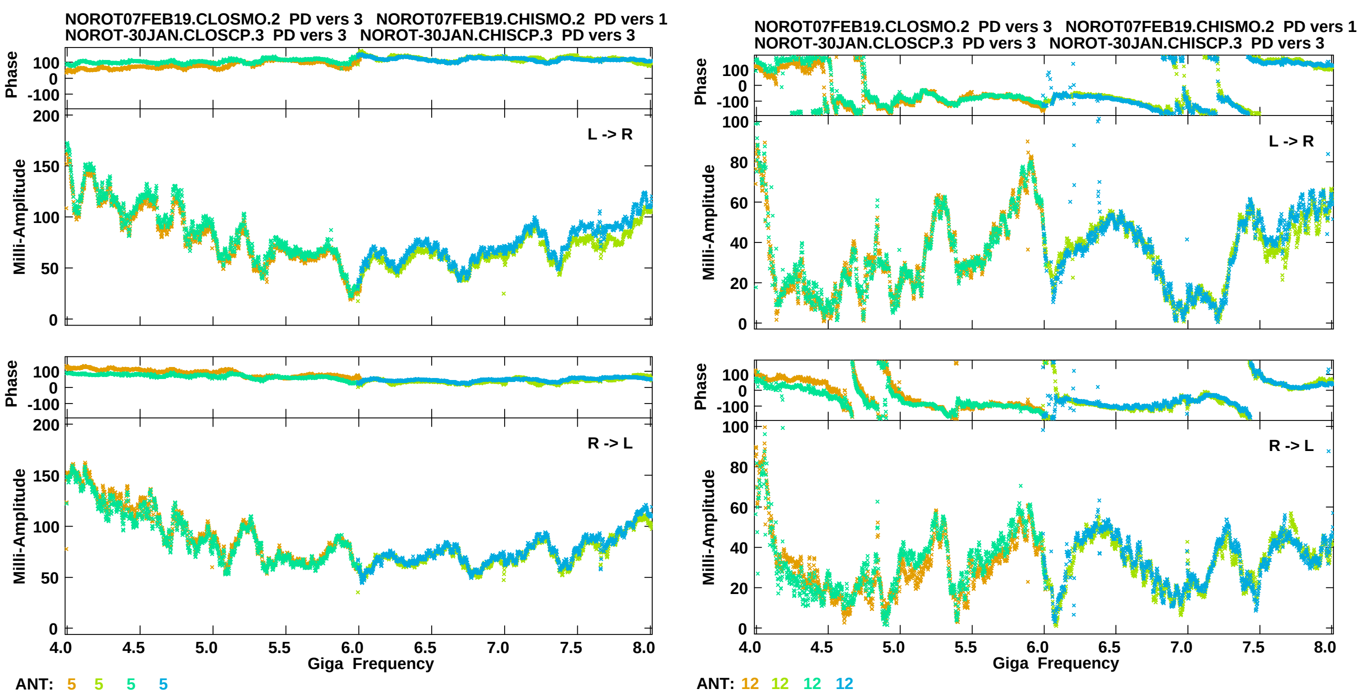

Figure 12: Showing the polarization stability at C-band, for antenna ea05 (left) and ea12 (right), between 2019 (light colors) and 2019 (dark colors). Ea05 has an 'old-style' hybrid, ea12 a 'new-style'.

7.4 X-band

No data were taken at X-band in 2019, so we investigate the stability for those antennas whose receivers were not changed between 2013 and 2020. Fig 13 shows the repeatability for a receiver which did not change antennas (receiver X-028 in ea27), and a receiver (X-022) which was in ea12 in 2013, and in ea17 in 2020. The repeatabity shown here over the 7 year period is typical over all receivers, with only three where the disagreement at any frequency was more than 2%. All three moved antennas between 2013 and 2020.

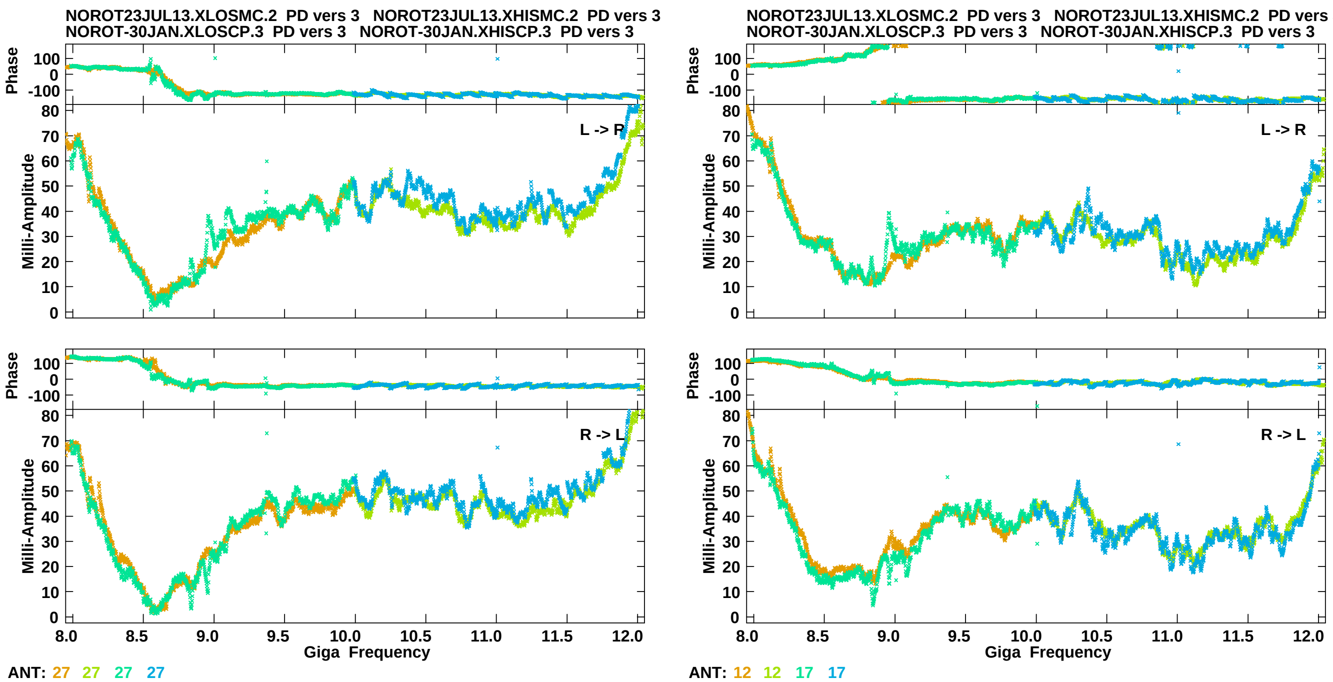

Figure 13: Showing the excellent polarization stability at X-band. The left panel shows receiver X-028, which was in the same antenna (ea27) in both 2013 and 2020. The right panel shows receiver X-022, which was in ea12 in 2013, and ea17 in 2020.

7.5 Ku-Band

Polarization data from only a single epoch (January 2020) has been taken. We can thus make no statements about stability.

8 Narrowband vs. Wideband Polarizers

In March 2011, the new X-band wideband polarizers were outfitted on just five antennas – ea06, 07, 14, 16, and 24. The initial polarimetry observations on that date thus give us a good comparison of the performance of the new wideband design compared to the old narrow-band design, which was optimized for good performance between 8.0 and 8.8 GHz. In Fig 14, we show the results for four new systems (ea06, 07, 14, and 24) and four old ones (ea01, 02, 04, and 05) over the range 8 to 9 GHz. It is immediately seen that the old polarizers are much better, with typical cross-polarization of just 1 – 2%, while the new, wideband designs, in the 8 – 8.8 GHz range, are poorer – and many times poorer at the low edge of the band. This is the cost of wide-band performance.

The clear difference seen in X-band is not evident at L-band, where we have, from the 2011 results, data from both the old narrowband designs and the new wideband designs, over the original VLA's frequency rnge of 1.3 to 1.75 GHz. These are shown in the right panel pair of the figure.

9 Discussion

The key results are that the absolute cross polarizations of the JVLA are below, or close to, the design goals of 5%, and that these polarizations are extremely stable over timescales of years, with typical changes of a few tenths of one percent, and maximum deviations of ∼2%. We also can conclude that, at least at L through X

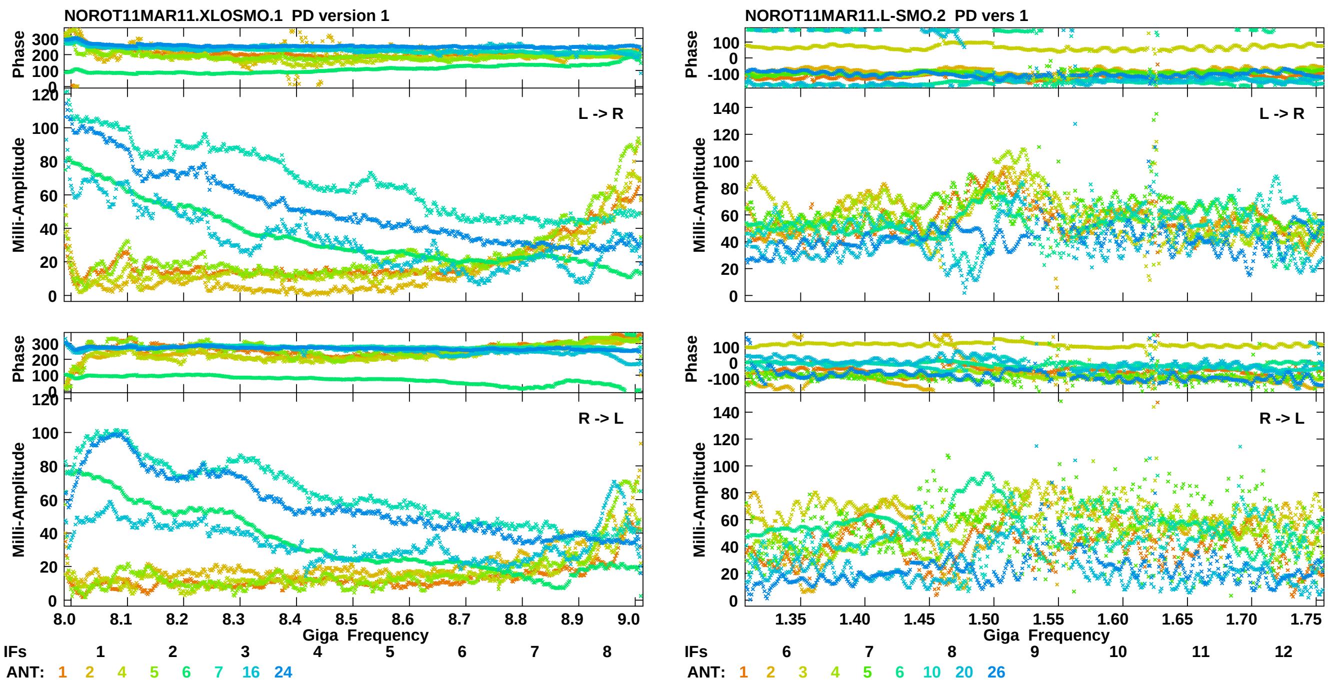

Figure 14: (Left) Showing the cross-polarization couplings for four old-style, narrow-band receivers, and four new-style, wide-band, receivers. The old designs (the original NASA Voyager receivers) on ea01, 02, 04 and 05, shown in the lighter colors, have much purer polarization characteristics over the 8.0 – 8.8 GHz range. (Right) Comparing the original L-band VLA polarizer to the new L-band wideband polarizer, from 2013 observations. In this case, the new wide-band polarizers (ea6, 10, 20, and 26 – the green and blue plots) are similar to the old, narrow-band design (ea 01, 02, 03, 04 and 04), seen in the lighter colors.

bands, the system polarization are greatly dominated by the receivers, with the antennas themselves (on-axis) contributing not more than a fraction of 1% to the system polarization.

These conclusions should make it possible to avoid the time-consuming process of determining antenna polarizations during the course of observations. Rather than having to find and observe an unpolarized source to determine the leakages for short observations where the parallactic angle rotation is insufficient, we could use tabulated values. It may also be possible to avoid the need for observation of a strongly polarized source to fix the cross-hand phases, as the antenna polarizations shown in this memo show remarkably repeatable cross-hand phases. This issue has not been investaged in any depth yet.

As noted in the introduction of this memo, there are two separate issues to consider – first the determination of absolute leakages, then the full matrix application. Both will be needed to achieve high-fidelity polarimetry. We will report on the second of these issues in a later memo.

The antenna rotation method for determining the 'D' terms does not require high system gain stability, since self-calibration can be employed to remove atmospheric and instrumental temporal fluctuations. It can thus be employed in any configuration, and in almost any weather. Indeed, the results shown here from 2019 and 2020 were highly affected by RFI, which is maximized by the low fringe rate which comes with C and D configuration observations. The data would have been much easier to handle, and the results continous over frequency, had the observations been taken in the B or A configurations. It should also be emphasized that this method requires only a single observation in each of the two array states – although we must remain mindful that, as the results for all antennas save the rotated one are based on a single baseline, a very strong, mostly unresolved and unpolarized source is needed. Fortunately, 3C84 at high frequencies, and 3C147 at low frequencies, are well suited.

However, the antenna rotation method, as implemented on the VLA, does suffer from one limitation – the antenna cannot be rotated, so we depend on the dominance of the receiver polarization over the antenna polarization for meaningful results. This may not be the case at higher frequencies, or for other arrays. It must also be mentioned that physically rotating the VLA's feeds is a difficult and labor-intensive process, and is likely not possible at all for the three highest bands (K, Ka, and Q), which are tightly packed in the VLA's vertex room.

This leads us to note that, for future arrays, accurate, fast, and reliable polarization calibration will be greatly benefitted by enabling (at least) one antenna in the array to rotate by a known angle (preferably 90 degrees) about the boresight, upon command[7]. It should be emphasized that the rotating antenna does not need to be one of the standard array antennas. A single 'calibration' rotateable antenna, with sufficient sensitivity over the frequency bands, would suffice to enable this method to be employed. Also, note that the polarization purity of this 'calibration' antenna is unimportant. Indeed, it could be argued that, since it is the cross-hand correlations that are utilized, a poorly polarized antenna might actually be desired.

10 Acknowledgements

Physically rotating the VLA's receivers (which weigh up to 150 pounds) is physically demanding work. We are very appreciative of the efforts expended by Craig Hennies, Dan Dillon, Jack Ramzel, Eddie Sanchez, and Ben Simkin in doing this. We also thank Chat Hull for his useful comments on an earlier draft.

11 Appendix

The D-terms are useful for signal analysis, but their relation to the antenna polarization performance, normally expressed in terms of the polarization ellipse, is not obvious. Here we show the connection.

The D-terms are defined such that D_{rl1} describes the voltage leakage from polarization 'R' to 'L' for the first antenna in the baseline. These terms are directly related to the antenna's polarization ellipse properties by:

$$D_{lr} = \tan\beta_r e^{2i\phi_r} \tag{21}$$
$$D_{rl} = \tan\beta_l e^{-2i\phi_l}. \tag{22}$$

The angles ϕ_r and ϕ_l are the orientations of the major axes of the polarization ellipses for the REP and LEP channels, respectively, in the antenna reference frame. The angles β_r and β_l are defined as

$$\beta_r = \pi/4 + \chi_r \tag{23}$$
$$\beta_l = \pi/4 - \chi_l \tag{24}$$

and physically represent the deviation of the antenna polarization ellipticity from perfect circularity. The angle $\chi = \arctan(b/a)$ $(b \leq a)$ is a measure of the ellipticity of the antenna polarization ellipse in the antenna frame of reference. Left elliptical polarization has positive ellipticity ($\chi_l > 1$), right elliptical polarization is negative ($\chi_r < 1$). Low antenna cross-polarization (nearly perfectly circular polarization) means that $\beta \ll 1$. As defined above, both β_r and β_l are positive real quantities. It can be shown that the ellipticity $\epsilon = b/a$ is related to the magnitude of the cross-polarization 'D' term by

$$\epsilon = \frac{1 - |D|}{1 + |D|} \tag{25}$$

[7] The entire reflecting structure, not just the receivers.